DESIGN OF THE SPOKE CAVITY ED&D INPUT COUPLER*

E. N. Schmierer†, K. C. D. Chan, R. C. Gentzlinger, W. B. Haynes, F. L. Krawczyk, D. I. Montoya, P. L. Roybal, D. L. Schrage, T. Tajima, LANL, Los Alamos, NM 87545, USA

Abstract

The current design of the Accelerator Driven Test Facility (ADTF) accelerator contains multiple β, superconducting, resonant cavities. Spoke-type resonators (β = 0.175 and β = 0.34) are proposed for the low energy linac immediately following the radio frequency quadrupole. A continuous wave power requirement of 8.5 – 211.8 kW, 350 MHz has been established for the input couplers of these spoke cavities. The coupler design approach was to have a single input coupler design for beam currents of 13.3 mA and 100 mA and both cavity β's. The baseline design consists of a half-height WR2300 waveguide section merged with a shorted coaxial conductor. At the transition is a 4.8-mm thick cylindrical ceramic window creating the air/vacuum barrier. The coax is 103-mm inner diameter, 75 Ohm. The coax extends from the short through the waveguide and terminates with an antenna tip in the sidewall of the cavity. A full diameter pumping port is located in the quarter-wave stub to facilitate good vacuum. The coaxial geometry chosen was based on multipacting and thermal design considerations. The coupling coefficient is adjusted by statically adjusting the outer conductor length. The RF-physics, thermal, vacuum, and structural design considerations will be discussed in this paper, in addition to future room temperature testing plans.

1 BASIC LAYOUT DECISION

Table 1 is the proposed makeup of the Accelerator Driven Test Facility (ADTF) linac cavity β's and power requirements for the low energy portion (6.7 – 109 MeV) [1]. The design approach for the low energy linac was to have a single input coupler design for both possible beam currents and all β's. The baseline design consists of a half-height WR2300 waveguide section merged with a shorted coaxial conductor. At the transition is a 4.8-mm thick cylindrical ceramic window creating the air/vacuum barrier. The coax has a 103-mm inner diameter and 75-Ohm impedance. Figure 1 shows the power coupler design and its features. Figure 2 is a cross-section that shows overall lengths.

Several options were considered for the basic structure layout. Based on our experience with the Accelerator Production of Tritium (APT) power coupler [2], we wished to retain its desirable features. These were 1) good pumping speed near the ceramic window, 2) a center conductor cantilevered off of a shorting plate that is easy to cool (this allows options for simple assembly and there is no weight on the window), 3) a window that is a separable piece from the coupler, and 4) it was a design that transmitted over 1 MW, CW on the test bench. The features that were undesirable were 1) the requirement of a tee connection and the resulting tee bellows which required an intricate joining technique, 2) a heavy and cumbersome unit, and 3) a high cost due to complexity.

The design selected is based on the KEK, TRISTAN normal conducting design for the APS cavity, which transmitted 300 kW to beam [3]. Compared to the APT design it still allows good pumping at the window, has a robust center conductor cantilevered off the shorting plate without the tee connection issues, has a window separable from the coax and waveguide, and is a simpler, lighter, lower cost design.

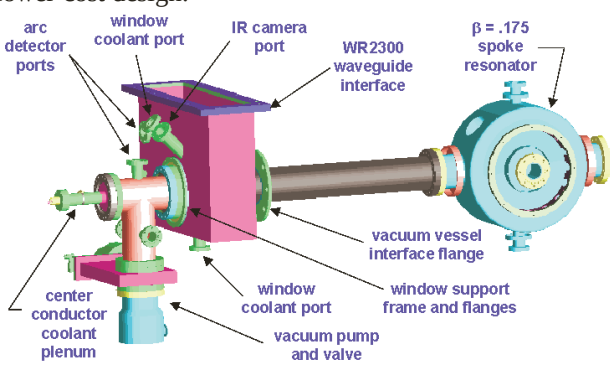

Figure 1: Schematic of the ADTF ED&D power coupler with a β = 0.175 spoke cavity

Table 1: Low-energy makeup of the proposed ADTF linac showing CW power requirements for the power coupler for two beam current options [1]

cavity β	spoke cavity type	cavities per section	13.3 mA beam current (kW)	100 mA beam current (kW)
0.175	2-gap	80	8.5	63.6
0.34	3-gap	36	28.2	211.8

* Supported by US DOE, NNSA and the Office of Nuclear Energy, Science and Technology

† schmierer@lanl.gov

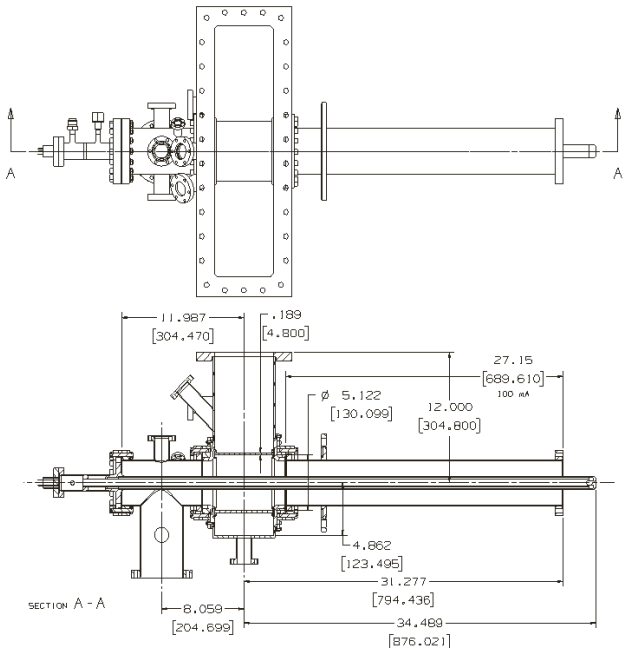

Figure 2: Detailed cross-section of the ADTF ED&D power coupler connected to a β = 0.175 spoke cavity (dimensions are in inches [mm])

2 MORE DESIGN DECISIONS

Besides the decision on the type of coupler some more features specific to this application had to be considered. For a favorable spoke resonator efficiency, small apertures are crucial. This did not allow coupling RF-power into the resonator from the beam-pipe, as is the standard for elliptical superconducting resonators. The point of connection between the power coupler and the resonator is the outside wall of the cavity. This location allows addition of the power coupler without requiring additional beam-line space (due to the 350 MHz frequency, the waveguide has however become the determining feature for cavity separation). A complication resulting from this choice is the direct connection of the coupler to the cavity volume, which results in a change of this volume and thus the resonant frequency of the cavity. For this reason the choice of the coupler port size and position had to be determined before the design of the resonator itself [4]. Also, the loading of the cavity due to the presence of the center conductor had to be accounted for in tuning the cavity frequency. A simple coaxial antenna coupling to the weak electric field had to be weighed against a more complex magnetic loop that couples to the much stronger magnetic field at the outside cavity wall.

One major concern about high power couplers is the potential for multipacting. For straight coaxial lines scaling laws can be used to estimate line sizes and impedance to avoid multipacting in the range of operation. If dangerous bands cannot be evaded, DC-biasing might have to be incorporated into the coupler design from the start, which adds to the complexity and thus cost of a design.

Another feature that we deem important for a trouble-free operation of a high power coupler is a vacuum pump port that allows controlling the vacuum level close to the RF-window of the coupler. Finally, the window RF-properties have been taken from previous experience with RF-windows for the APT project [5].

2.1 Electric Coupling vs. Magnetic Coupling

Spoke resonators and λ/4 resonators so far have been used for low current applications and thus low input power. Due to the large magnetic field at the outer cavity body wall, magnetic loop coupling typically has been proposed for these resonators. For higher power levels the thermal management of such loops especially in a cryogenic environment are undesirable and expensive. Thus the possibility of a standard coaxial antenna coupler was investigated. The required external Q values for the nominal operation at various beam currents from 13.3 to 100 mA were determined assuming a 30 degree phase advance and a active spoke cavity length of 0.1m (Table 2). Simulations with MAFIA [6,7] indicate the sufficiency of the electric coupling. The method was verified in the lab with a fixed coaxial antenna on an ANL 2-gap spoke resonator [8].

Table 2: Nominal Q_{ext} for various currents and E_{acc}

	13.3 mA	**100 mA**
5 MV/m	1.42×10^6	1.89×10^5
7.5 MV/m	2.13×10^6	2.83×10^5

2.2 Choice of Coaxial Line Size

The main consideration of the coaxial line size selection is multipacting. Multipacting levels can be scaled from known levels, considering the line diameter (~ d^4), the frequency (~ f^4) and the impedance (~ Z) of the line [9]. Comparing these levels to the nominal operation power levels allows selecting a proper coaxial line. Table 3 gives the lowest seven single-point multipacting levels for the CERN LEP2 couplers and for two potential line choices with 50 and 75 Ω impedance. Since the lowest-β cavity has limited outer wall space the size chosen is a compromise decision. A smaller coaxial line would give undesired multipacting levels at operation power levels and larger coaxial lines would not fit onto the lowest-β cavity.

Table 3: Single-point multipacting in coaxial lines

Order	**CERN**	**103 mm**	**100 mm**
	352 MHz 75Ω	350MHz 75Ω	350MHz 50Ω
7	48 kW	47 kW	28 kW
6	52 kW	51 kW	30 kW
5	88 kW	86 kW	51 kW
4	176 kW	172 kW	102 kW
3	234 kW	229 kW	136 kW
2	448 kW	438 kW	259 kW
1	640 kW	626 kW	371 kW

The center column was our geometry of choice. Multipacting levels above the thicker black line would be reached for the lowest-β spoke resonators in our design at 63.6 kW, CW. Levels above the thicker broken line would be reached at the highest-β in our design, 211.8 kW, CW. We feel that the levels of 6th and 7th order should not be a limiting factor of operation for this coupler. Tests on a room temperature test stand will show if this coupler is feasible at the highest-β. If there is a limit, we could either implement DC-biasing into the design or increase the coupler size for the higher-β cavities, which can accommodate a larger diameter coupler.

2.3 Vacuum Pump Port

The major concerns of the vacuum pump port size and location are gas conductance and space considerations due to interference with the cryostat. The preferred position is the λ/4 stub with a full diameter and no screening. The RF-mismatch due to the port is easily compensated by the short position in the stub. At 350 MHz the vacuum pump-port is a cut-off tube that does not leak RF-power into the vacuum pump if the pump is properly spaced on the port.

3 COUPLER RF-PROPERTY MODELING

The starting point of the optimization was the design of a geometry that fulfills the performance specifications in terms of power transmission at the operating frequency and meets the considerations of the previous section. Modifications were then made based on space and thermal considerations. The modeling and results presented in this paper are for 95% pure alumina RF-window. A higher purity ceramic is currently being considered.

3.1 The Modeling Tools

We used a set of complementary 3D simulation programs for the RF-design. The design started with HFSS [10] and was then continued with MAFIA [7] and MWS [11], where each program had its strengths on subsets of the issues to solve. The RF-results were also transferred to thermal and stress analysis tools concurrently to get an integrated understanding of the coupler performance.

3.2 Performance Requirements

The performance requirements are listed in Tables 1 and 4. They were derived from our experience with generators and coupler performance for the APT accelerator.

Table 4: RF-performance requirements for the coupler

match frequency	350 MHz	
return loss	< -30 dB	at f_{match}
bandwidth	> ± 1 MHz	at –20 dB
return loss at the vacuum pump	< -60 dB	at pump flange

3.3 Optimization Procedure

Some basic geometry parameters are fixed, driven by the frequency (WR2300 waveguide) or the considerations of the previous section. The first order optimization was done by variation of the coaxial and waveguide shorts. The vacuum pump port also influences the match. Its position was used for some final tuning adjustment. The coaxial short predominantly influenced the matching frequency, while the waveguide short and the vacuum port position had a stronger influence on the return loss. The optimal lengths of the quarter-wave and waveguide stubs were close to the nominal quarter-wave length in each guide. Table 5 gives the list of the most important geometry and RF-performance numbers.

Table 5: Geometry and RF-parameters for the optimized spoke cavity coupler

coax diameter	103 mm	CERN dimensions
coax impedance	75 Ω	
waveguide	WR2300	
window-type	cylindrical	
window-material	95% pure (ε = 9.1, tan δ = 0.0027)	
window OD	139.7 mm	
thickness	4.8 mm	
transition	½-height waveguide to λ/4 stub	
coax short	305.5 mm to window center	
waveguide short	130 mm to window center	
vacuum port	140 mm to waveguide top	
coax-length	1196.7 mm from short to tip	
pump flange	450 mm to coax center	
orientation	45 degrees from spoke	
f_{match}	350.1 MHz	
S11	-45 dB	
bandwidth	± 11 (3) MHz at –20 (30) dB	

Figure 3 shows a MWS model of the waveguide-to-coax transition of the coupler geometry. In Figure 4 are the S-parameters from the modeling. The green curve is the return loss of the transition. The red curve is the transition of power to the cavity and the blue curve shows the return loss through the vacuum port.

3.4 Interaction between Coupler and Cavity

The coupler attachment to the outer cavity wall does influence the cavity frequency. In simulations with MAFIA the coupler tip positions relative to the cavity for operation with 13.3 and 100 mA beam current have been determined. Table 6 contains the resulting tip positions and the frequency change between the two settings that have to be compensated by the cavity tuner.

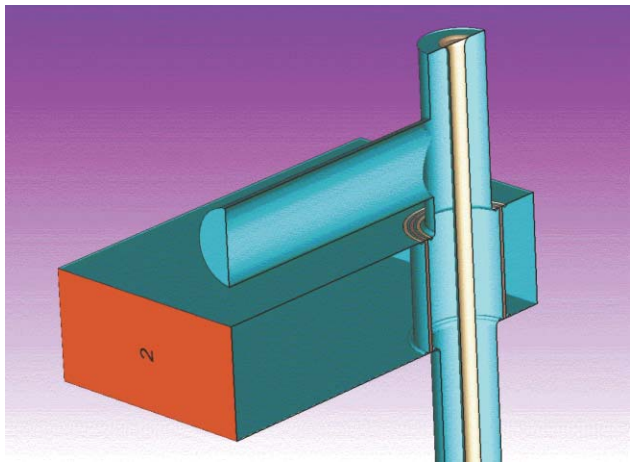

Figure 3: A cutaway view of the coupler MWS model

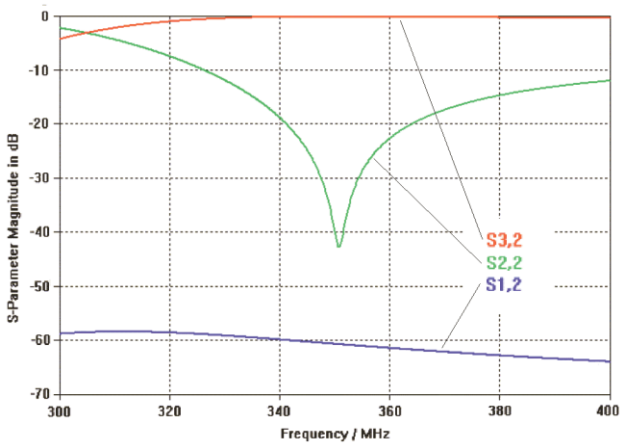

Figure 4: S-parameters for the optimized geometry

Table 6: Tip positions relative to the cavity wall and frequency change between high and low current operation

	tip position	df
13.3 mA	20 mm withdrawn	N/A
100 mA	7 mm withdrawn	23 kHz

3.5 Sensitivities

For tuning and for fabrication purposes the change of matching frequency and return loss with variation in short positions and other geometrical tolerances are studied. Results are not available at this moment.

3.6 RF-losses as Input for a Thermal Evaluation

RF-losses are currently being calculated as input for a thermal evaluation of the coupler. The integrated losses on the center conductor have been calculated analytically (for a straight coaxial line) and numerically for the actual coupler geometry. Also the distribution of the dielectric losses in the alumina window have been calculated. Table 7 lists the results of the total power to be removed for the two beam currents, corresponding to a power transmission of 8.5 kW and 63.6 kW respectively.

Table 7: Total losses on coax center conductor and the dielectric RF window for the $\beta = 0.175$ section

	13.3 mA	100 mA
Coax-center, Straight Coax	23 W	77 W
Coax-center, Actual Coupler	23.8 W	79.2 W
Coax-short	8.2 mW	61 mW
Window Ceramic	0.7 W	5.3 W

4 MECHANICAL AND THERMAL PROPERTIES OF THE COUPLER

The fabrication of the power coupler is planned via an outside vendor and will be based on end-product drawings and a specification. The vendor will be responsible for the final design; the coupler shall be able to handle 500 kW, CW (~2 x 211.8 kW, CW) thermally and electrically. However, a high power acceptance test will only be required up to 150 kW, CW (~2 x 63.6 kW, CW). Our goal with the current structural and thermal analysis was to determine if the requirements put on the design are reasonably achievable.

4.1 Structural Analysis

We are requiring the center conductor be made of OFE Cu with a cantilevered design. The bending stress and deflection with the coupler in the horizontal orientation is a concern due to its 1.20-m length. The maximum stress at the antenna/short joint is 2600 psi with a 0.073-in. deflection of the tip due to a gravity load.

The long length makes dynamic motion a possible concern also. Analysis of just the outer Cu sleeve of the center conductor resulted in a fundamental frequency of 13.4 Hz. Using random vibration measurements from the APT/LEDA tunnel [12], the lateral rms tip displacement was calculated to be 39.3-μin.

The mass of the power coupler assembly is approximately 63 kg with the pump and gate valve. This is centered approximately at the RF-window center.

4.2 Thermal Analysis

The coolant path for the center conductor will be the same as the APT coupler with air or helium as the coolant. Figure 5 shows the coolant path in the center conductor.

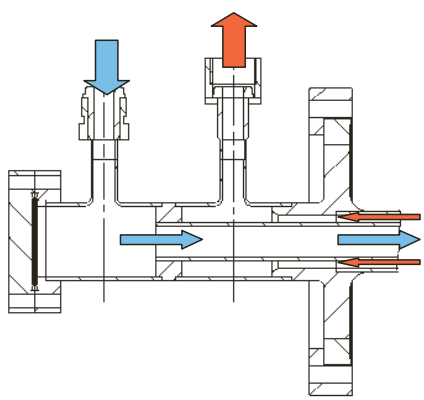

Figure 5: Center conductor coolant inlet and outlet paths

An upper limit of 3 g/s has been set for the coupler based on the maximum amount available at the Room Temperature Test Bed (RTTB) [13]. At this mass flow rate the maximum center conductor temperature is 85˚C at 500 kW, CW. The outer conductor will not be actively cooled for room temperature testing or beam testing on LEDA.

An estimate of the thermally induced movement of center conductor tip relative to cavity was performed. A change of tip location due to 0.037-in. of outer conductor contraction plus 0.015-in. of center conductor expansion results in 0.052-in. of tip insertion towards the cavity. For a 100-mm outer conductor diameter, this increases Q_{ext} by approximately 14 %. Results for the 103-mm diameter are not available at this moment.

4.3 Vacuum Analysis

For analysis of vacuum, the window ceramic was assumed the major gas contributor. Two layouts were considered with the use of a 300 l/s turbo pump. One was with the vacuum pump port located between the cavity and the waveguide and the other with the vacuum port on the room temperature outer conductor as in Figure 1. There was little effect on the ultimate pressures between the pump locations, therefore the pump was put on the quarter-wave stub to minimize length of outer conductor from the waveguide to the cavity.

5 FUTURE WORK

Engineering drawings and a statement of work for procurement of the prototype coupler are in progress. We plan to have vendor quotations in October 2001 with the intention of awarding a contract in late 2001 for 3-4 coupler assemblies. The procurement approach is to purchase a "turn key" design. Delivery is anticipated in mid to late 2002 with high power acceptance testing on the RTTB occurring in late 2002.

Acceptance testing will consist of conditioning to 150 kW, CW and a 24-hr. test at this power. A 212 kW, SW test with a sliding short is also planned. A few units will then be tested on the RTTB up to 500 kW, CW to characterize multipacting and determine whether this design can be used for the entire low-energy section without biasing. For this testing, minor modifications of the existing RTTB will be required. A spoke coupling cavity made of OFE Cu will be used to test two power coupler assemblies together.

6 ACKNOWLEDGEMENTS

We would like to acknowledge and thank Brian Rusnak for his continued involvement and helpful discussions regarding the spoke cavity power coupler development at LANL.

7 REFERENCES

[1] Robert Garnett, "Revised strawman S2 design for ADTF cost comparison basis," LANSCE-1 memo 01-034.

[2] Eric Schmierer et al., "Results of the APT RF Power Coupler Development for Superconducting Linacs", this workshop.

[3] Mitsuo Akemoto et al. "High Power Input Coupler with a Cylindrical Alumina Window", Proceedings of the 1991 Particle Accelerator Conference, San Francisco, USA (1991).

[4] Frank Krawczyk et al., "Design of a Low-β Spoke Resonator for the AAA Project", Proceedings of PAC 2001, Chicago, USA (2001).

[5] APT Accelerator Topical Report, LA-CP-94-48, March 1994.

[6] Pascal Balleyguier, "A Straightforward Method for External Q Computation", Particle Accelerators, Vol. 57, pp 113-127, 1997.

[7] http://www.cst.de/products/mafia/mafia.htm

[8] Frank Krawczyk, "RF Simulations and Room - Temperature Measurements of the ANL 2-Gap Spoke Cavity", LANL internal report.

[9] Joachim Tuckmantel et al., "Improvements to Power couplers for the LEP2 Superconducting Cavities", Proceedings of the 1995 Particle Accelerator Conference, Dallas, USA (1995).

[10] http://www.ansoft.com/products/hf/hfss/index.cfm

[11] http://www.cst.de/products/mws/mws.htm (Microwave Studio)

[12] Stephen Ellis, "APT/LEDA Tunnel Floor Random Vibration Measurements," Proceedings of the 2001 Particle Accelerator Conference, Chicago, USA (2001).

[13] Jack Gioia, et al., "A Room Temperature Test Bed for Evaluating 700-MHz RF Windows and Power Couplers for the Superconducting Cavities of the APT Linac," Proceedings of the 1999 Particle Accelerator Conference, New York City, USA (1999).